DOI: 10.1007/s12541-012-0248-3

Development of the Exoskeleton Knee Rehabilitation Robot Using the Linear Actuator

KyuJung Kim[1], MinSung Kang[2], Younsung Choi[3], HyeYoun Jang[3], Jungsoo Han[4], and Changsoo Han[3,#]

1 Department of Intelligent Robot Engineering, Hanyang University, Haengdang 1-dong, Seongdong-gu, Seoul, South Korea, 133-791
2 Department of Mechatronics Engineering, Hanyang University, Haengdang 1-dong, Seongdong-gu, Seoul, South Korea, 133-791
3 Department of Mechanical Engineering, Hanyang University, Haengdang 1-dong, Seongdong-gu, Seoul, South Korea, 133-791
4 Department of Mechanical System Engineering, Hansung University, Samseon-dong 2-ga, Seongbuk-gu, Seoul, South Korea, 136-792
Corresponding Author / E-mail: cshan@hanyang.ac.kr, TEL: +82-31-400-4062, FAX: +82-31-406-6398

KEYWORDS: Knee, Continuous Passive Motion(CPM), Arthroplasty, Linkage, Rehabilitation

This study aimed to develop a robot for effective knee joint rehabilitation. A kinematic approach was used to make exoskeleton robot joints to have the same range of motion (ROM) as that of human knee joints, and a robot exoskeleton was proposed to enable the wearer maintain a proper posture during rehabilitation therapy. This robot is generally used for the rehabilitation therapy for knee lesion patients (e.g., after knee replacement arthroplasty and cruciate ligament reconstruction), where the patients usually lie down wearing this robot. The alignment of the knees and body is a critical factor for the success of the therapy. Considering the rehabilitation therapy posture, the robot was manufactured with a kinematic structure different from that of the existing robots for knee rehabilitation therapy. In this study, the kinematic mechanism of the knee rehabilitation robot was described, and the actuator for the robot was selected by measuring the human knee joint motion and torque. Thus, an exoskeleton robot that is significantly different from the existing knee rehabilitation robots was developed.

Manuscript received: February 14, 2012 / Accepted: May 1, 2012

1. Introduction

Robot for knee rehabilitation exercise are largely divided into two types. The first type supports the human body, and the second assists the human body. The supporting type supports patients who have lost their gait ability due to paraplegia or brain injury, and helps in their gait training. This robot supports the human body according to the synchronous signals from the human body or the force and torque signals generated between the robot and the human body. The assisting robot, which is used for rehabilitation therapy, is driven in the preset rehabilitation mode instead of using the signals from sensors. This study aimed to develop the assisting robot for knee rehabilitation therapy.[1,2]

Continuous Continuous passive motion (CPM) is mostly used for knee rehabilitation therapy that uses assisting robots. This device is used for the rehabilitation of patients with knee joint diseases (e.g., after knee replacement arthroplasty or cruciate ligament reconstruction). With the advent of the aging society, more and more people are suffering from osteoarthritis and have implants in their knees via knee replacement arthroplasty. Rehabilitation is essential after knee replacement arthroplasty, and joint immobilization therapy is conventionally conducted. Nevertheless, it was recently reported that therapy can be more efficient if the knee joints are allowed to move intermittently at the very least, because it helps the patients' adaptation and the recovery of the joint motion range.[1] The recovery of the joint motion range is the most important part for knee joint rehabilitation, and efficient for reducing edema and mitigating swelling after the operation.[2,3]

The efficacy of rehabilitation therapy via CPM, however, is currently under clinical debate. Compared with physical modalities, the CPM therapies show only short-term rehabilitation effects and do not lead to further advantages. In addition, there is a problem regarding the alignment between the human knee joints and the CPM joints. The CPM must be driven in the same ROM as that of the human joints, and the posture must not influence the knee joints. In the previous study using the motion capture device and an electrogoniometer, the CPM and human knee joints had different ROMs, where most CPM joints had a lower ROM than the actual knee joints. In addition, the patient's posture significantly influenced the results.[4,5]

In the study, the theoretical background for knee joints was examined, and four-bar links, which are similar to the human knee

joints, were used to address the difference in ROM between the human knees and the robot. Based on the recognition that the human knee joints consist of two cruciate ligaments in the four-bar link structure, they were kinematically analyzed. Using the analysis data, an exoskeleton joint was developed so that it has the similar ROM to that of the human knees (-5° to 135°).[6] In addition, a knee rehabilitation therapy robot structure for proper rehabilitation therapy posture was proposed.

2. Exoskeleton design

2.1 Shape of the human knee joint link

The human knee joint consists of a medial transfemoral joint, a lateral transfemoral joint, and a patella. Its motions include flexion and extension on the sagittal plane, and internal and external rotation on the horizontal plane. The internal and external axes of rotation for flexion and extension are not fixed. Rolling and sliding occur on the femoral condyles. The moving path of the axis is called "evolute" or "instant center of rotation." The movement of the rotation axis biomechanically changes the length of the internal moment arm.[7]

Fig. 1 shows the human knee joint seen on the sagittal plane. The cruciate ligament is attached to the femur and tibia. The attachment and halting points of the cruciate ligament and other ligaments appear as a four-bar link shape. AB shows the anterior cruciate ligament (ACL), and CD, the posterior cruciate ligament (PCL). AD and BC are the distances from the ligament attachment point (origin) to the halting point (insertion) in the tibia and femur, respectively. **I** is the instant center of rotation, at which the cruciate ligaments intersect, and is helical in the **J** shape, as shown in Fig. 2.[8]

In this study, the approach was based on the ligament structure rather than the shape of the femur. This was because the femur has spherical surfaces due to the medial and lateral femoral condyles. However, the surfaces of the two condyles are different and thus move differently.

In this study, the four-bar link structure of the ligament was analyzed; the center of rotation was estimated according to the knee flexion; and the analysis results were reflected on the exoskeleton joint design of the robot.

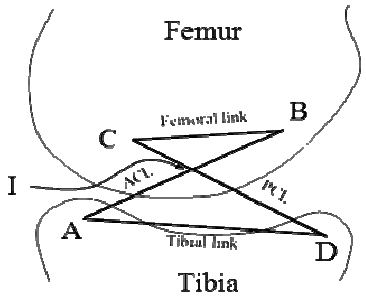

Fig. 1 Picture of a human left knee with the lateral femoral condyle removed, exposing the cruciated ligaments (reference No). The diagram of the four-bar ABCD is superimposed, representing the anterior (AB) and posterior (CD) cruciated ligaments, the femur (CB) and tibia (AD) rigid bond links. I represents the instant center of flexion

2.2 Exoskeleton knee joint design

First, the four-bar link structure of exoskeleton was formed based on the analyzed human four-bar link structure. The trajectory of the center of rotation for the human knee joint was varied proportionately to develop the exoskeleton knee joint. It was based on the fact that the trajectory of the instant center of rotation of the human endoskeleton knee joint varies as the lateral distance increases.[9-11] The screw-home rotation due to the medial and internal femoral condyle surfaces was not considered because only the motions on the sagittal plane was considered for the effects of knee rehabilitation therapy.

Fig. 3 kinematically shows the human knee joint. The anterior cruciate ligament is l_4, the posterior cruciate ligament is l_2, and the ligament attachment points of the femur and tibia are l_1 and l_3, respectively. The human knee joint was modeled in vectors. The change in the center of rotation was observed. This type, called the "Chebyshev's linkage," has a 1 degree of freedom.[12] The monocentric and polycentric hinges are also used for exoskeletons, but they show a bigger ROM difference from the human knee joint with larger knee flexion angle.[13]

$$\vec{L}_1 + \vec{L}_2 = \vec{L}_4 + \vec{L}_3 \tag{1}$$

$$\begin{bmatrix} \ell_1 \\ 0 \end{bmatrix} + \begin{bmatrix} \cos\theta_2 & -\sin\theta_2 \\ \sin\theta_2 & \cos\theta_2 \end{bmatrix} \begin{bmatrix} \ell_2 \\ 0 \end{bmatrix} = \begin{bmatrix} \cos\theta_4 & -\sin\theta_4 \\ \sin\theta_4 & \cos\theta_4 \end{bmatrix} \begin{bmatrix} \ell_4 \\ 0 \end{bmatrix} + \begin{bmatrix} \cos\theta_3 & -\sin\theta_3 \\ \sin\theta_3 & \cos\theta_3 \end{bmatrix} \begin{bmatrix} \ell_3 \\ 0 \end{bmatrix} \tag{2}$$

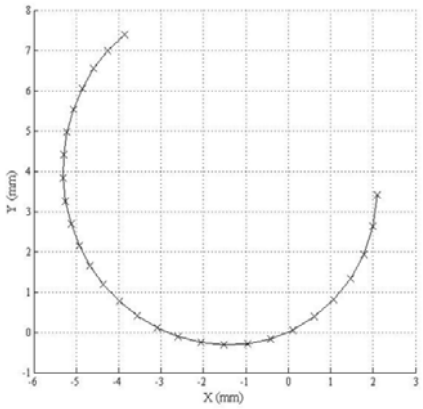

Fig. 2 Instant center of flexion of the human knee joint

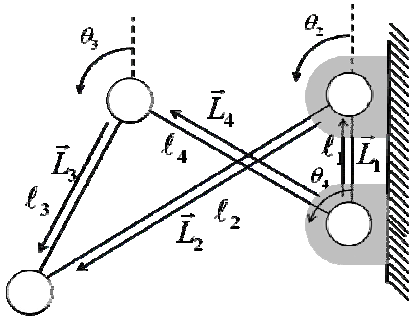

Fig. 3 Exoskeleton knee joint designed by using four-bar linkage

Accordingly, the endoskeleton of the human knee joint and the exoskeleton of the robot were considered different in the approach. The four-bar link structure of the ligament was examined, and the Chebyshev's linkage structure was used to develop the exoskeleton joint similar to the human knee joint. We designed the exoskeleton CPM knee joint taking into consideration that the human knee joint is an endoskeleton, therefore equations (1) and (2) are derived.

2.3 Design considering the linear actuator

The ROM of the knee joint was examined to determine that of the robot. The ROM of the robot was set at 135° because the flexion range of the human knee joint is 135°. To control the robot within this ROM, an actuator was chosen as follows.

When When the existing knee rehabilitation device, CPM, is fixed on the body, the patient is put in an uncomfortable posture because the CPM occupies a large space. We aimed to minimize the device volume to ensure a comfortable posture for the patient. The actuator and its position were determined so that the patient could either lie or sit. The linear actuator was used to generate translational motion on the femur. An additional link was installed to convert the translational motion of the linear actuator to the rotational motion of the robot knee joint.[14]

The device was designed so that it could allow limited stroke length change in the linear actuator and a 135° motion range for the robot joint. It was also designed so that the extended stroke would not touch the knee. Fig. 4 shows the overall simplified version of the robot. Inputs are delivered to the link via the linear actuator. Subordinate bar l_5 rotates within the 135° range to realize the flexion of the knees.

The kinematic part that generates rotational motion through the translational motion of the linear actuator is divided into two parts: the upper and lower parts. Link l_9 converts the translational motion into rotational motion according to the linear actuator, and becomes the actuation link for the entire link part. Fig. 5 is the link of the upper part, which is a four-bar link that has a single degree of freedom. The lower part is connected to the upper part and helps the rotation of the final link. The reciprocating translational motion of the linear actuator was considered in the design, and it moves just like the knee joint, with flexion and extension. The designed link part had a single degree of freedom and was modeled as follows. From the modeling equation, the rotational motion of the link generated by the translational motion of the linear actuator and the relative change of the initial angle to the final value can be identified.

The upper part is comprised of four-bar linkage system as in Fig. 5 and modeled as equation (3) and (4). The equations for the lower part are equations (5) and (6). part comprised of four-bar linkage system as on Fig. 5 and modeled as equation (3) and (4), Lower part equation is (5) and (6).

$$\vec{L}_{10} + \vec{L}_6 = \vec{L}_9 + \vec{L}_8 \tag{3}$$

$$\begin{bmatrix} \ell_1/2 \\ \ell_{10} \end{bmatrix} + \begin{bmatrix} \cos\theta_6 & -\sin\theta_6 \\ \sin\theta_6 & \cos\theta_6 \end{bmatrix} \begin{bmatrix} \ell_6 \\ 0 \end{bmatrix} = \begin{bmatrix} \cos\theta_9 & -\sin\theta_9 \\ \sin\theta_9 & \cos\theta_9 \end{bmatrix} \begin{bmatrix} \ell_7 \\ 0 \end{bmatrix} + \begin{bmatrix} \cos\theta_8 & -\sin\theta_8 \\ \sin\theta_8 & \cos\theta_8 \end{bmatrix} \begin{bmatrix} \ell_8 \\ 0 \end{bmatrix} \tag{4}$$

$$\vec{L}_4 + \vec{L}_3/2 + \vec{L}_5 = \vec{L}_1 + \vec{L}_6 + \vec{L}_7 \tag{5}$$

$$\begin{bmatrix} \cos\theta_4 & -\sin\theta_4 \\ \sin\theta_4 & \cos\theta_4 \end{bmatrix} \begin{bmatrix} \ell_4 \\ 0 \end{bmatrix} + \begin{bmatrix} \cos\theta_3 & -\sin\theta_3 \\ \sin\theta_3 & \cos\theta_3 \end{bmatrix} \begin{bmatrix} \ell_3/2 \\ 0 \end{bmatrix} + \begin{bmatrix} \cos\theta_5 & -\sin\theta_5 \\ \sin\theta_5 & \cos\theta_5 \end{bmatrix} \begin{bmatrix} \ell_5 \\ 0 \end{bmatrix} = \begin{bmatrix} \ell_1 \\ 0 \end{bmatrix} + \begin{bmatrix} \cos\theta_6 & -\sin\theta_6 \\ \sin\theta_6 & \cos\theta_6 \end{bmatrix} \begin{bmatrix} \ell_6 \\ 0 \end{bmatrix} + \begin{bmatrix} \cos\theta_7 & -\sin\theta_7 \\ \sin\theta_7 & \cos\theta_7 \end{bmatrix} \begin{bmatrix} \ell_7 \\ 0 \end{bmatrix} \tag{6}$$

Since the ROM of the robot joint is already known, the calculation can be made inversely. θ_9 of link l_9 can be determined

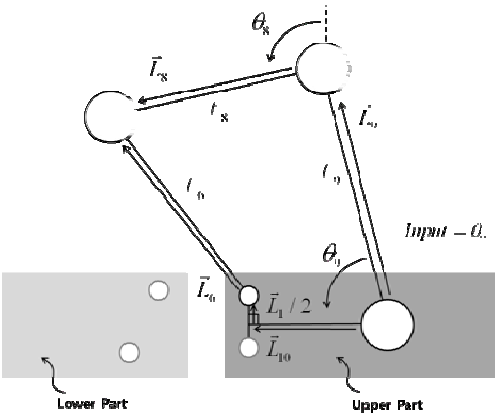

Fig. 5 Lower linkage structure of the knee rehabilitation robot mechanism

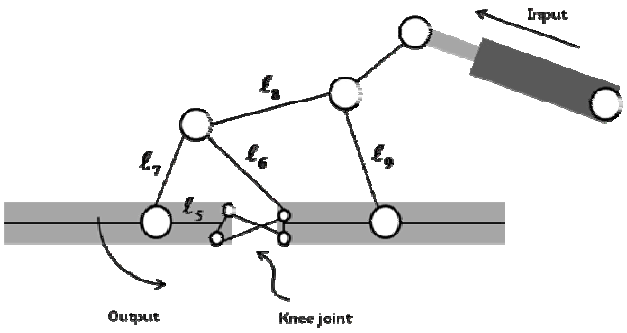

Fig. 4 Structure of the knee rehabilitation

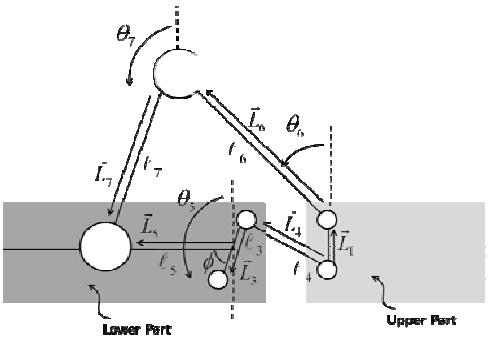

Fig. 6 Upper linkage structure of the knee rehabilitation robot mechanism

when the robot joint rotates from 0 to 135°. The knee joint angle value is inputted first, and it becomes the value of θ_5. Since the values of θ_3 and θ_5 are fixed, θ_3 and θ_5 can be calculated using the modeling equation (6). The known values of θ_3, θ_4 and θ_5 can be used to calculate θ_6, and θ_9 can be finally obtained. The relative displacement difference between θ_9 and θ_5 can be determined via this process, and the link length is optimized to minimize the displacement difference.[17]

3. Optimization of the link

The relative difference between θ_5 and θ_9, which is known, is the core part of this robot development.

It is important because the minimal motion of the linear actuator within the flexion range of the human knee joint can supplement the linear actuator's limited stroke length and can minimize the interference with the human body. Therefore, the value of θ_9 could be calculated from θ_5 using the modeling equations, and we sought the value with the least relative displacement compared to the initial value. The objective function for this optimization is expressed as equation (7).

$$\frac{\Delta\theta_9}{\Delta\theta_5(0-135^\circ)} \tag{7}$$

The link length is the most influential factor for the final optimized value. The links are formed in diverse angles, according to their length and the objective function is obtained when the link lengths are determined. The link length is a design parameter for this optimization.

The genetic algorithm was used to find the optimal link combination. Darwin's genetic algorithm was developed according to the theory of evolution, where the optimal solution is found based on the principles of the survival of the fittest and natural selection. The principle of this algorithm has a structure similar to that of a chromosome. The operations, including selection, crossover, and mutation, are repeatedly conducted within the strings to find a better solution. The dominant genes survive, whereas the recessive genes die out during the evolution.[15]

The flexion of the robot from 0 to 135° was optimized. The optimal solutions for the links were found with the optimization, under the following conditions:

$$\begin{aligned} \text{Subject to}: \quad & 50 \le L_6 \le 80, 40 \le L_7 \le 80 \\ & 60 \le L_8 \le 200,\ 60 \le L_9 \le 250 \end{aligned} \tag{8}$$

MATLAB® Optimization Toolbox was used to implement the genetic algorithm with a population set at 100. The roulette method, where the individual elements are selected in proportion to the fitness, was used for the selection operation. The scattered method, where the selection is randomly conducted, was used for the crossover operation.

With the genetic algorithm, the value converged to a minimum when the operation was conducted to the 100th generation. There was no further improvement, and the optimal solution was obtained as follows.

Table 1 Optimal link length

Links	Length(mm)
L6	55.04
L7	40.643
L8	123.998
L9	135.195

4. Calculation of the torque for knee rehabilitation

A linear actuator was used to drive the robot. The minimum actuator torque for lifting the lower leg was calculated. The torque was calculated using the data based on the anthropometrical characteristics, including body mass and height. The muscle-power-measuring equipment Kin-Com was used to measure the torque during the actual continuous passive exercise, for comparison. The results were used as an important index to determine the robot actuator's torque. Simulations were conducted with the results.

4.1 Exoskeleton knee joint design

The data for the knee model in this study were obtained using 11 musculotendinous units. The geometric leg model was obtained using the cadaver data. Fig. 3 shows the human-body model with an average height of 1.75 m and a weight of 746 N. Fig. 3 shows the length, mass, and location of the center of gravity for each part on a sagittal plane.

The location of the center of gravity of the lower leg was calculated to determine the knee joint moment.[16]

Assuming that segment 1 as the shank and the segment 2 as foot, each moment arm of the center of mass of segment 1 and 2 are x_1 and x_2 respectively. The mass of each segment is W_1 and W_2 respectively. According to the conventional calculation method of the moment of force, the center of mass point can be derived by equation (9). So as to find out the critical design requirements of the proposed system, the minimum nominal torque can be estimated through equation (10).

$$M_O = (W_1 + W_2)x_{cg} \tag{9}$$

$$x_{cg} = \frac{x_1 W_1 + x_2 W_2}{W_1 + W_2} \tag{10}$$

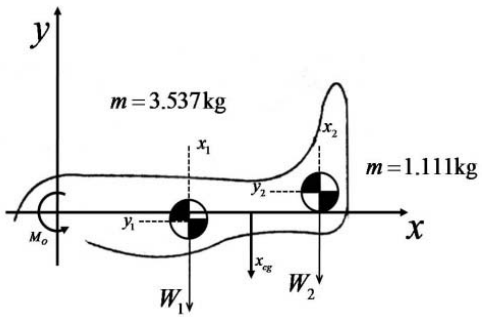

Fig. 7 Configuration of the center of mass of the lower leg

4.2 Measuring of the human torque using the muscle-measuring equipment

In this experiment, the torque of the knee joint generated during an actual knee joint rehabilitation exercise was calculated. The muscle-measuring equipment Kin-Com was used, as in Fig. 8. Kin-Com has a load cell on its link, which measures. The weight of the lower leg. The lengths of the link which are the moments arms, ranged between 200~240mm according to the subjects. The torque can be determined using the weights measured on the moment arm and load cell. In a continuous-passive-exercise mode, the equipment conducts isokinetic motion with a speed of 10rpm. Five sets of these tests were conducted 10 times with 13 robust males. The subjects had an average age of 28.4, an average weight of 76kg, and an average height of 173.2㎝, which were similar to the human measurement data. The result of this experiment shown that torque value regarding movement time and angle of knee joint through Kin-Com equipment. Fig. 9 is mapped by polynomial curve fitting using equation(11). The highest torque measured was 22.4Nm (Fig. 9), and the average of the highest torques was 14.45Nm. The lowest torque was 8.55Nm, which significant gap from the highest torque. These results were similar to the torque values that were calculated using the human-body model. Since people have different body figures, the highest torque was applied to the robot, and safety factors were considered.

$$f_i = \sum_{j=0}^{m} a_j x_i^j \tag{11}$$

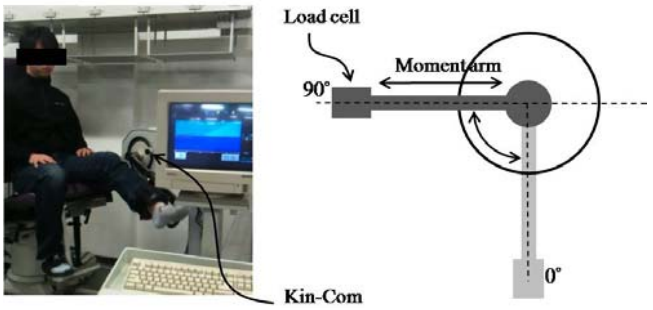

Fig. 8 (right) ROM of Kin-Com (left) Experiment

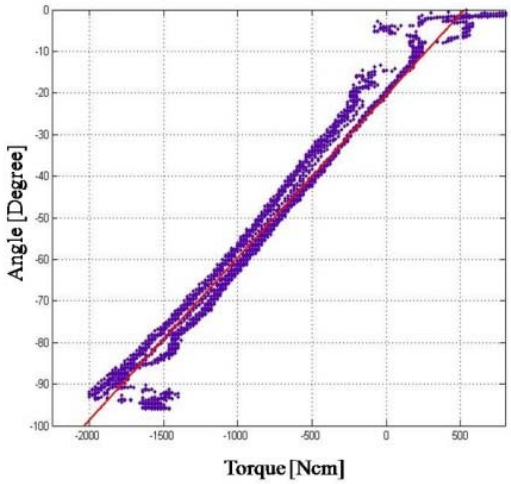

Fig. 9 The highest torque value through the Kin-Com experiment

4.3 Calculation of the joint torque via dynamic simulation

To consider the actuator performance of the designed system, we measured the force generated when the human lower leg was lifted via simulations. The linear actuator length was determined considering the system's size, and the actuator force was not considered. The simulation results will be used to determine the linear actuator force. The dynamic analysis program Recurdyn® was used for the simulation. The weight of the human leg model was considered for the link that was connected to the lower leg.

In this simulation, we aimed to calculate the force required for the linear actuator when the system in operation and this force was used to determine actuator specifications for the system. According to the simulation results, the measured force was 251.96N.

The optimal link combination was previously identified through the optimal link design, but the stroke of the linear actuator was not considered. This was because the size of the linear actuator is determined according to the link length. According to the genetic algorithm, the length of the linear-actuator suitable for the optimally designed link length was determined. We examined the relationship between the stroke of the linear actuator, which represents linear displacement and the flexion from 0° to 135° which represents the rotational displacement. The maximum stroke length of the actuator was determined according to the resulting values.

5. Result

In this study, an exoskeleton knee joint with the same instant-center-of-rotation trajectory as that of the human knee joint was developed. It was designed in such a way that the actuator was not positioned on the same axis as the human knee, and a linear actuator was used to lift the lower leg. The purpose of this design was to consider the patients going through rehabilitation therapy after knee replacement arthroplasty or other knee joint operations. The knee joint was designed with the Chebyshev's linkage structure, with the same ROM as the human knee joint to mitigate the burden of knee rehabilitation therapy and to ensure efficient ROM rehabilitation.

The linear actuator conducts translational motion, which is converted to rotational motion through the link structure. In this kinematic structure, the interference between the human femur and

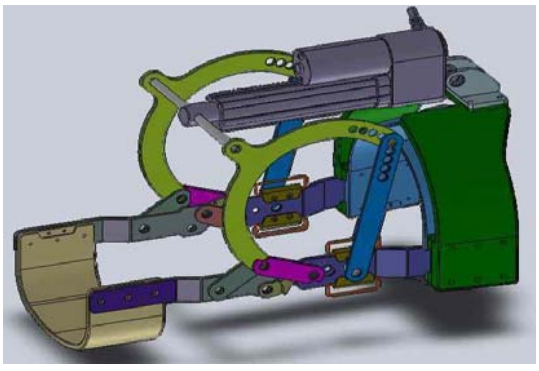

Fig. 10 Final Design

the linear actuator, and the limited stroke length of the linear actuator were addressed via optimization. After optimization, the 135° flexion of the robot showed a muscle change in linear-actuator stroke length, which was only a few millimeters. The average knee joint torque was estimated from the cadaver leg model data to determine the torque for driving the actuator, and it was reflected on the actuator selection after the verification via the actual experiment.

6. Conclusion

This study aimed to improve the convenience and portability of the existing fixed-type CPM. The actuator was placed on the femur, which does not have the same axis as the knee to ensure comfortable rehabilitation therapy. With the existing fixed-type CPM, the patient has to maintain an uncomfortable posture while undergoing rehabilitation therapy due to its bulky structure. The human knee joint did not align with the robot joint, depending on the posture. In this study, a structure was proposed to solve these problems.

The structure was proposed to minimize the negative effects during rehabilitation therapy after knee operation, and the structural problems were solved using the optimization tool. If wearable or humanoid robots are studied with sufficient understanding of the human knees, it is expected that this robot structure will be used in a wide range of robot applications as well as rehabilitation therapy.

ACKNOWLEDGEMENT

This research was supported by the Happy tech. program through the National Research Foundation of Korea (NRF) funded by the Ministry of Education, Science and Technology (No. 2011-0020938).

REFERENCES

1. O'Driscoll, S. W. and Giori, N. J., "Continuous passive motion (CPM) : Theory and principles of clinical application," Journal of Rehabilitation Research and Development, Vol. 37, No. 2, pp. 179-188, 2000.
2. Brosseau, L., Milne, S., Wells, G., Tugwell, P., Robinson, V., Casimiro, L., Pelland, L., Noel, M. J., Davis, J., and Drouin, H., "Efficacy of continuous passive motion following total knee arthroplasty: A metaanalysis," Journal of Rheumatology, Vol. 31, No. 11, pp. 2251-2264, 2004.
3. Evans, E. B., Eggers, G. W. N., Butler, J. K., and Blumel, J., "Experimental Immobilization and Remobilization of Rat Knee Joints," The Journal of Bone and Joint Surgery, Vol. 42, No. 5, pp. 737-758, 1960.
4. Bible, J. E., Simpson, A. K., Biswas, D., Pelker, R. R., and Grauer, J. N., "Actual knee motion during continuous passive motion protocols is less than expected," Clin. Orthop. Relat. Res., Vol. 467, No. 10, pp. 2656-2661, 2009.
5. London, N. J., Brown, M., and Newman, R. J., "Continuous passive motion: Evaluation of a new portable low cost machine," Physiotherapy, Vol. 85, No. 11, pp. 610-612, 1999.
6. Smidt, G. L., "Biomechanical analysis of knee flexion and extension," Journal of Biomechanics, Vol. 6, No. 1, pp. 79-92, 1973.
7. Parenti-Castelli, V., Leardini, A., Di Gregorio, R., and O'connor, J. J., "On the Modeling of Passive Motion of the Human Knee Joint by Means of Equivalent Planar and Spatial Parallel Mechanisms," Autonomous Robots, Vol. 16, No. 2, pp. 219-232, 2004.
8. Walker, P. S., Kurosawa, H., Rovick, J. S., and Zimmerman, R. A., "External knee joint design based on normal motion," Journal of Rehabilitation Research and Development, Vol. 22, No. 1, pp. 9-22, 1985.
9. Bertomeu, J. M. B., Lois, J. M. B., Guillem, R. B., Pozo, P. D., Lacuesta, J., Mollá, C. G., Luna, P. V., and Pastor, J. P., "Development of a hinge compatible with the kinematics of the knee joint," Prosthetics and Orthotics International, Vol. 31, No. 4, pp. 371-383, 2007.
10. Nielsen, D., Blocker, L., and Pardo, N., "Coordinated planar mechanisms to approximate the three dimensional motion of the knee," Journal of Medical Devices, Transactions of the ASME, Vol. 3, No. 3, Paper No. 034501, 2009.
11. Tashman, S. and Anderst, W., "In-vivo measurement of dynamic joint motion using high speed biplane radiography and CT: Application to canine ACL deficiency," Journal of biomechanical engineering, Vol. 125, No. 2, pp. 238-245, 2003.
12. Ottaviano, E., Ceccarelli, M., and Tavolieri, C., "Kinematic and Dynamic Analyses of a Pantograph-Leg for a Biped Walking Machine," International Conference on Climbing and Walking Robots, pp. 561-568, 2004.
13. Kurosawa, H., Walker, P. S., and Abe, S., "Geometry and motion of the knee for implant and orthotic design," Journal of Biomechanics, Vol. 18, No. 7, pp. 487-499, 1985.
14. Schiele, A. and Van Der Helm, F. C. T., "Kinematic design to improve ergonomics in human machine interaction," IEEE Transactions on Neural Systems and Rehabilitation Engineering, Vol. 14, No. 4, pp. 456-469, 2006.
15. Lim, H., Hwang, S., Shin, K., and Han, C., "The application of the Grey-based Taguchi method to optimize the global performances of the robot manipulator," Intelligent Robots and Systems (IROS) IEEE/RSJ, pp. 3868-3874, 2010.
16. Shelburne, K. B. and Pandy, M. G., "A musculoskeletal model of the knee for evaluating ligament forces during isometric contractions," J. Biomechanics, Vol. 30, No. 2, pp. 163-176, 1997.
17. Kim, K. J., Kang, M. S., Choi, Y. S., Han, J., and Han, C.,

"Conceptualization of an exoskeleton Continuous Passive Motion(CPM) device using a link structure," IEEE International Conference on Rehabilitation Robotics (ICORR), pp. 1-6, 2011.